# A manufacturing driven design methodology to lightweighting of the structural elements of a permanent magnet electrical machine rotor

**Jill Miscandlon[1], Abbas Kazemi-Amiri[2], Stephen J. Forrest[3], Xiao Chen[3], Daniel Harper[3], Alasdair McDonald[4], Geraint W. Jewell[3]**

[1] National Manufacturing Institute Scotland, University of Strathclyde, Glasgow G1 1XH
[2] Department of Electronic & Electrical Engineering, University of Strathclyde, Glasgow G1 1XH
[3] Department of Electronic and Electrical Engineering, University of Sheffield, Sheffield, S1 3JD
[4] Institute for Energy Systems and Mechanical Engineering Discipline, School of Engineering, University of Edinburgh, EH9 3FB

Corresponding author: Jill Miscandlon (e-mail: jill.miscandlon@strath.ac.uk).

**ABSTRACT** It is common practice for electrical machines to be designed with a focus predominantly on the electromagnetic performance. The mechanical design is then subsequently undertaken to meet various mechanical performance criteria, with this finalised design then passed on for manufacture. In many cases, the manufacturing constraints have not been taken fully into consideration during the electromagnetic or more particularly the mechanical design and hence some changes are required to the design to make it manufacturable. This in turn can lead to a non-optimal machine being manufactured. If manufacturing constraints and opportunities are regarded as key quantitative inputs to the design process, not only can these post-design changes be minimised, but benefits of the manufacturing process can be exploited to produce a superior product. This paper proposes a methodology to fully integrate the mechanical design and manufacturing process routes into electrical machine design and illustrates its utility within the context of light-weighting of a permanent magnet rotor for an aerospace electrical machine. Within the proposed methodology, several alternative configurations of the rotor are considered with applicable manufacturing routes identified at the initial stages of design and an analytical design procedure to fulfil the application and performance criteria is developed. Different manufacturing materials and constraints as well as the impact of manufacturing process are identified to be embedded into the design procedures. Finally, the paper demonstrates an application of this methodology together with a discussion of the features which offer promise in achieving economically lighter weight design through integration of manufacturing into the design procedure.

**INDEX TERMS** electrical machine, rotor dynamics, lightweight, structural design, manufacture

## I. INTRODUCTION

This paper describes a design methodology for the structural elements of an electrical machine rotor that encompasses both the design opportunities and manufacturing options at the initial stage of design inception. Whereas the design of the active elements of the machine is critical in realizing a competitive power density, i.e. those elements that have functional role in generating electromagnetic torque, the non-active or structural elements also have a key role. By way of example, the design study reported in [1] included a detailed mass audit of a 100kW high-speed aerospace starter-generator that employed a combination of high performance soft magnetic materials and direct oil cooling of the windings to achieve an overall machine continuous operation power density of 4.4kW/kg. In the final machine design, 47% of the final machine mass was contributed by structural elements.

In straightforward terms, this suggests that there is equal scope to drive forward power densities through optimisation of the design of the structural elements. This necessarily involves embracing new materials and manufacturing routes. Bringing the manufacturing considerations into the early design iterations not only allows for the optimal manufacture of components, but uses the advantages of individual manufacturing methods to open up the design space and allow for radical changes from a traditional electrical machine design. An alternative design concept spoked hub for the the study reported in [1] is presented in FIGURE 1 **Spoked hub design** for the purpose of illustration of various major components of an electrical machine.

The design of a complete rotor assembly for a high-performance permanent magnet machine involves establishing an acceptable trade-off between electromagnetic
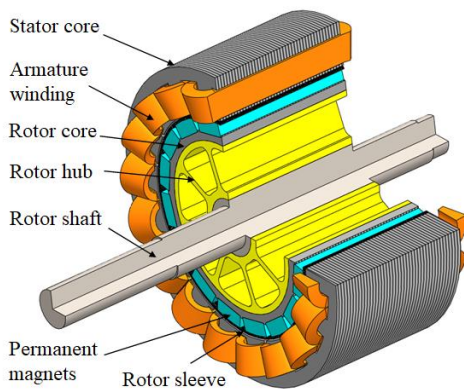
FIGURE 1 Spoked hub design

performance, mass, structural integrity, rotor-dynamic behaviour and manufacturing considerations such as cost and precision of process control. Rotors which operate at high peripheral speeds, i.e. >200m/s, pose particular challenges as their design becomes increasingly dominated by mechanical rather than electromagnetic considerations [2]. In order to achieve the highest possible power density for a given stator arrangement, and usually, but not always, the highest efficiency, considerable design effort is put into maximising the air gap magnetic flux density. It is also usual to attempt to minimise the rotor mass through judicious selection of materials and dimensions. However, both these design objectives, which are often regarded as being the primary electromagnetic design objectives, are desirable design outcomes rather than strictly essential criteria, which must be met. These primary design objectives must be achieved while simultaneously meeting many essential requirements for the rotor in which there is little or no leeway for trade-off:

- Ensure that the rotor magnets are maintained in contact with the rotor core across the full operating speed range, including for any overspeed specifications.
- Ensure that any containment sleeve employed to retain the rotor magnets operates below the material design stress limit for all combinations of rotor speed and operating temperature.
- Ensure that the rotor magnets and/or the rotor core are not subjected to excessive mechanical compressive stress from the containment sleeve during manufacture or at any point in the temperature and speed operating envelope of the machine.
- Ensure that the vibration from a combination of unbalanced magnetic pull and out-of-balance forces do not exceed some specified limit.
- Ensure sufficient margin between the first critical speed of the rotor and the maximum operating speed (including any overspeed considerations).

- Reduce the level of rotor electromagnetic losses, which comprise core loss and induced eddy current magnet loss, to a level which can be sustained thermally (this aspect of behaviour being closely coupled to the stator design).
- Avoid irreversible demagnetisation of the rotor magnets under the worst-case temperature and overload current conditions.
- Incorporate a means to ensure that the rotor can be dynamically balanced to a high precision.
- Shear stress limit - referenceable design guidelines for margin/safety factor [3].
- The shaft design must ensure that the losses in the rotor (e.g. from induced eddy currents in the rotor magnets or rotor core loss) can be dissipated to the surrounding ambient or into a cooling fluid. This is likely to be achieved through a combination of heat conduction within the rotor (including along the shaft to some external sink) and from convention from the various surfaces.

With the possible exception of reducing the rotor electromagnetic losses, all of the above requirements demand compliance with some threshold of performance/behaviour. In many cases, there is little merit in further exceeding these requirements recognising that many of the thresholds have been set with regard to ensuring the component or assembly will exhibit the requisite ageing behaviour over its design lifetime by appropriate specification of a safety factor or design margin. It is also apparent from these requirements that many are in direct conflict with each other and/or the performance objectives of air gap flux density and rotor mass.

It is also important to note that manufacturing considerations have the potential to impact on the rotor design in several ways:

- The material physical properties which underpin the selection of the form and dimensions of various elements may well be highly influenced by the processes employed in component manufacture, e.g. forging versus machining from bar stock in the manufacture of the shaft, work-hardening of material through cold-forming etc.
- Geometrical tolerances may influence the precision of the control which can be exercised over assembly and resulting performance, e.g. arising interference stresses.
- The cost effectiveness of any given manufacturing route will be dependent on factors including number of units per year, availability of supply chain, and the ratio of the raw material weight used to manufacture the part to the final part weight.

One example of the nature of the trade-offs involved in rotor design is the potential to use the rotor core (also commonly referred to as the rotor 'back-iron') as a structural element. The principal electromagnetic role of the rotor core is to

provide a low magnetic reluctance path for the rotor permanent magnet flux. To a first approximation, the rotor core is exposed to a static magnetic field. However, in a practical machine, there is usually some degree of localised fluctuations in the magnetic flux in the rotor core due to a combination of armature reaction field and stator slotting permeance variation modulating the localised working point of the rotor magnet. These localised flux variations will give rise to induced eddy currents and hence loss in the rotor core, the extent of which is related to the electrical conductivity of the core material and the rotor geometry, in particular whether it is manufactured from a solid single-piece or from a stack of laminations. A stack of electrical steel laminations (usually <0.5 mm) which are either adhesively bonded across the full face or welded together at a few points around the outer periphery are generally regarded as being elements which cannot be relied on to carry any meaningful mechanical loads. In contrast, a rotor core manufactured from a high-strength ferromagnetic alloys can be integral to the structural design of the rotor and in some cases eliminate the need for a rotor shaft and/or hub. However, since a solid rotor core will tend to result in markedly larger eddy currents than its laminated counterpart, considerable attention must be paid to minimising this parasitic rotor core loss to avoid excessive heating of the rotor structures.

In order to retain surface mounted magnets and/or improve the mechanical strength of the rotor structure, a high strength overwrap sleeve is often employed on the outer surface of the rotor. Typical sleeve materials include carbon fibre or a non-magnetic alloy, such as Inconel [3], [4]. Since the sleeve is required to deliver the retaining force over the entire speed range of the rotor, a degree of pre-load is required to negate the self-loading effect on the sleeve. However, it is important to recognise that application of radial pre-stress to the magnets and the underlying rotor core is not without its perils. Thus, as is the case in the proceeding analysis, it is necessary that this additional stress on the underlying rotor structure be taken into account at the design stage of the rotor structural components.

To avoid irreversible demagnetisation of the rotor magnets under the worst-case temperature and overload current conditions, an appropriate thermal design with accurate temperature prediction on the rotor magnets need to be performed to calculate the worst-case temperature. This thermal design needs to be carried out with a complete electrical machine rather than the rotor system alone, as the rotor magnet temperature is subject to not only the rotor losses but also the stator winding losses and the cooling approach used in the stator. Whereas the conventional thermal analysis usually uses lumped parameter thermal network with empirical heat transfer coefficients [6], nowadays the thermal analysis employs computational fluid dynamics approach to determine the heat transfer coefficients between different types of mediums (such as liquid/solid and air/solid) before performing the temperature prediction using the lumped parameter thermal network or thermal finite element analysis [7]. Then, the worst-case

temperature of the rotor magnet at load condition will be used to analyse the irreversible demagnetisation risk of the permanent magnets.

As noted previously, the majority of electrical machines have been historically designed with an emphasis on the electrical, mechanical, and thermal performance. The design is then iterated to best meet the specified performance criteria, with this finalised design of the active region then passed onto a manufacturer to fabricate. In cases where the manufacturing constraints have not been taken into consideration during the design, it is commonplace that changes are required to be made to the optimised design to make it manufacturable, leading to some compromise in performance. If manufacturing is considered as an input variable to the design process, not only can these post-production changes be eliminated, but advantages of the manufacturing process can be taken to produce a superior product. This paper will aim to develop a methodology for a fully integrated design and manufacturing process route, with an outline of the methodology given in FIGURE 2.
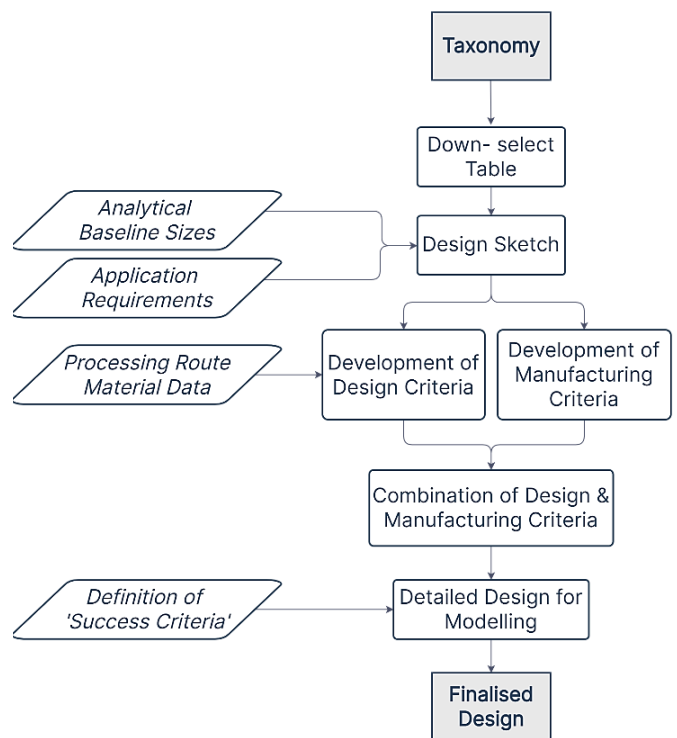
**FIGURE 2 Methodology outline**

## II. Literature Review

In this section, the state-of-the-art literature regarding the lightweighting of electrical machines' rotors will be presented. The lightweighting of the electrical motors and generators can be realised through modifications of both the electromagnetically active and non-active parts of a machine. In this regard, the state-of-the-art of lightweighting of electrical machines (EM) from different points of view, including electromagnetic, thermal, and mechanical and dynamics, as well as cost and manufacturing aspects are

reviewed. Furthermore, due to the wide range of utilisation of electrical motors and generators, the lightweighting of electrical machines in different industrial applications will be discussed too.

The work on reducing non-active material mass can be split into understanding loads, suggestions of design approaches and use of materials.

### A. Load modelling in rotating electrical machines

Similar to the other rotating machinery systems, electrical machines are subject to a number of operational loads, including the centrifugal loads, which is even more significant in the high-speed electrical machines as in vehicle and aerospace applications. However, the analysis of the rotor structure of the electrical machines are uniquely more complex because of the superposition of the mechanical loads such as torque and centrifugal forces, the air gap electromagnetic shear and normal stresses on the rotor circumference, thermal stresses [6], [7], and the dynamically induced vibration and noise due to manufacturing, installation or design imperfections.

Many of the forces acting on an electrical machine rotor are common to all rotating machinery, e.g. out-of-balance forces, gyroscopic forces, forces transmitted from a moving platform etc. However there are some additional forces resulting from electromagnetic interactions which must be quantified, and in some cases, taken into account. The torque ripple by an electrical machine can be reduced to very low levels if required by the end application, e.g. to <1% in electric power steering systems. In general terms, reducing torque ripple usually involves some modest compromise in average torque density and hence many permanent magnet machines have some level of residual torque ripple which is typically a few percent of average torque. This toque ripple is a combination of so-called cogging torque and harmonics in the excitation torque. One feature of torque ripple is that the excitation frequencies can be many multiples of the rotational frequency. By way of example, in a 48-slot, 8-pole permanent magnet machine, the dominant cogging torque frequency component is at 48 times the fundamental rotational frequency. There are some studies attempting in reducing the torque ripple, for instance the magnet pole shape design for ripple minimisation using analytical flux density expressions [10].

Mass imbalance is one of the main excitations for a rotor system. The resultant centrifugal force rotates synchronously with the rotor rotation, and hence the rotor rotation frequency needs to be kept away from the natural frequencies of the rotor system in the design stage. One unique feature of the rotor system of a permanent magnet synchronous machine is that the rotor of a typical PM machine is assembled up from a large number of separate individual components, which can include many hundreds of small individual magnet pieces if significant segmentation of the magnet poles is necessary to manage induced losses [11]. The tolerances of all the rotor components can stack up significantly, resulting in a large mass imbalance. Rotor balance standards were introduced to

mitigate the mass imbalance to acceptable levels for various applications, such as G2.5 for aerospace application based on ISO 21940-11:2016 [12].

The imbalance is considered in the unbalanced response analysis (vibration analysis), when there is a resonance point within the operation speed range. However, if there is no such resonance point below the max operation speed, we do not need to run the unbalanced response analysis. The unbalanced magnetic pull (radial force) analysis will be conducted in 2D electromagnetic FEA, and then the frequency order of the dominant unbalanced magnetic pull will be checked to see whether there is a chance to excite a resonance below the max operation speed. If this is not possible, then no further unbalanced response analysis will be needed. If it is possible, then the unbalanced response analysis will be run with both electromagnetic force excitation and the imbalance excitation [13].

Vibration of EMs are caused by internal and external sources that can interact simultaneously. Vibration dissipates energy, reduces the efficiency, can cause machine failure and produces unwanted noise. Distorted (uneven) air gap field due to eccentricity and magnetic flux change of the air gap basically give rise to unbalanced magnetic forces (UMF)). The uncoincidental rotor and stator axes and mass imbalance are among the internal causes of UMF. In order to avoid excess vibrations, design standards restrict the eccentricities to some permissible values [14].

Considering the various rotor components are made of different materials which have different coefficients of thermal expansion (CTE), the rotor exhibits a non-uniform thermally induced stress that can impact the effective stiffness of all the rotor components. Besides, the high rotor temperature can degrade the modulus of the rotor materials. Therefore, the rotor dynamics performances can theoretically be affected by thermal expansion. Zhuo et al. [15] investigated the influence of the thermal expansion on the natural frequencies of a gas turbine rotor, by performing the thermal analysis, mechanical stress analysis and then the modal analysis under the pre-stressed conditions. It was found that the error caused in the natural frequencies by neglecting the thermal expansion effect can be 4%. M. Zheng et al. analysed the thermal expansion effect on the natural frequencies of a micro gas turbine rotor system with a surface mounted permanent magnet machine [16]. The carbon fibre wrapping direction impact was considered in the thermal stress analysis. It was reported that by neglecting the thermal expansion effect, the error caused in the natural frequencies can be 8%. However, the rotor systems in both papers operate at high temperatures from 200°C to 500°C which can cause a relatively large degradation in the material modulus.

The structural and mechanical components of the EMs require sufficient strength to accommodate with the cyclic loads, which are imposed on them over the machine's lifetime. The cyclic loads can cause fatigue damage in the components such as shafts and bearings, which gives rise to machine's failure. Particularly in high speed machines, inappropriate selection of the rotor mass and inertia can

impose excessive loads on the bearing and reduce their fatigue life [17]. Fatigue damage is important to be investigated where some innovative machine designs are concerned. For instance, E. Sikanen et al. investigated the fatigue damage analysis within the rotor decks of a sleeveless embedded magnet machine design. They highlighted the necessity of considering the combined thermo-mechanical stresses in damage estimation analysis [18].

The motor design must take into account the resonance frequencies of the motor to shift the critical frequencies away from the motor's operating speed to at least ±10% [19]. For dynamic analysis of EMs rotor, possibly modelling of all components that may influence the vibration modes has to be taken into account, although the analysis complexity may increase. The relevant examples are the gyroscopic effect imposed by the bearing deformability that can introduce low order vibration modes [20] and the increased rotor hub stiffness by pre-stressed sleeves for retaining magnets [5].

## B. Materials

In the case of light weighting, Eastham et al. [21] have demonstrated use of novel material in the non-active structural part of a novel axial flux machine for aircraft drive application, including plastic and carbon fibre reinforced epoxy resin. The former is used as support disks for windings and magnets, whereas the latter is chosen for the shaft of chassis.

Koch et al. [22] studied the use of the soft magnetic compounds (SMC) and composite plastic to reinforce the steel shaft for the lightweight design and manufacturing of high performance electrical motors. Jean-Sola et al. [23] investigated the opportunities for lightweighting, using the composite materials with different fibre orientation patterns instead of steel for wind turbine generators.

For the selection of materials stated above, the feasibility of utilising these with various manufacturing methods has been considered. Titanium is applicable to a wide range of processes, including forging [24], casting [25], radial forging [24], and spinning [26]. Steels alloys are applicable to most manufacturing processes, although the yield strength obtained can greatly vary from 1420 MPa for a forged component [27] to 210 MPa for an extruded component [28]. For completeness, this paper also considers that use of aluminium, inconel, and magnesium alloys through a variety of processing routes. Before deciding on the material and manufacturing route, it is important to note that there will be limitations on the conditions in which the material can be processed using a certain route. For example, titanium is formable using the spinning process, but due to the microstructure of this material, the spinning process needs to be conducted at high temperature, typically in the region of 600−800 °C [29], with research being conducted into the use of laser-assisted spinning for difficult to deform, high strength alloys [30].

## C. Design Approaches

Design of modern electrical machines with lightweight and high-performance characteristics is of important interest due to their extensive applications. While the electromagnetic design is viewed in a systematic perspective, the mechanical design is predominantly approached from a component-oriented approach, in order to fulfil the machine's performance [31] and [32]. One route for innovation in the design of mechanical elements of electrical machines is to look at the designs of similar rotating systems, such as gas and wind turbines. One specific example is in [33] where the authors designed and modelled a lightweight electrical generator (for an airborne wind turbine) using composite material structure inspired by that from a flywheel design by [34].

From the design optimisation viewpoint, some recent studies have dealt with the review of the existing methods and techniques and tried to organise them into a distinct framework for the more optimal design. With a focus on the software selection, Duakaev et al. [35] have collected the tools used in the EM discipline and their application for machine design and optimisation.

In a more holistic approach, Bramerdorfer et al. [36] investigated the techniques for evaluating machine designs and its optimisation from an electromechanical standpoint. They provide a high-level definition of optimisation problem and the search-space technique, applied to EM science. With an approach to multi-physics (electromechanical, mechanical/structural, thermal), material and manufacturing process design, Lei et al. [37] reviewed the design optimisation methods and practices for EMs. They attempted to build frameworks for system-level and robust optimisation, and showed case study examples of their proposal implementations. Nevertheless, robust optimisation can have the downside of performing a considerable amount of simulations to consider the uncertainty in the input (design) parameters, such as material properties, geometry, manufacturing route and assemblage.

The performance and efficiency model along with the design methodology and cost optimisation of two powertrain configurations, including the electrical machine, converter and mechanical transmission is presented by [38] and [39] respectively. The selection of the optimal power train mechanical parts is based on the performance requirements. Having selected the powertrain, then from a database of EMs the optimal electrical machine design is sought through an objective function involving material and manufacturing cost.

Design for X (DfX), where X can be a range of activities such as manufacture, assembly, remanufacture and life-cycle, is a well-known process which has been in practice since the 1970's. The DfX process uses a range of simple criteria to question and critique the function and design of components, with the aim of reducing part count, production and assembly time, and any difficulties that may lead to quality issues in the final component [40]. There is a BSI standard available which gives high level criterion which should be taken into account when using the DfX process
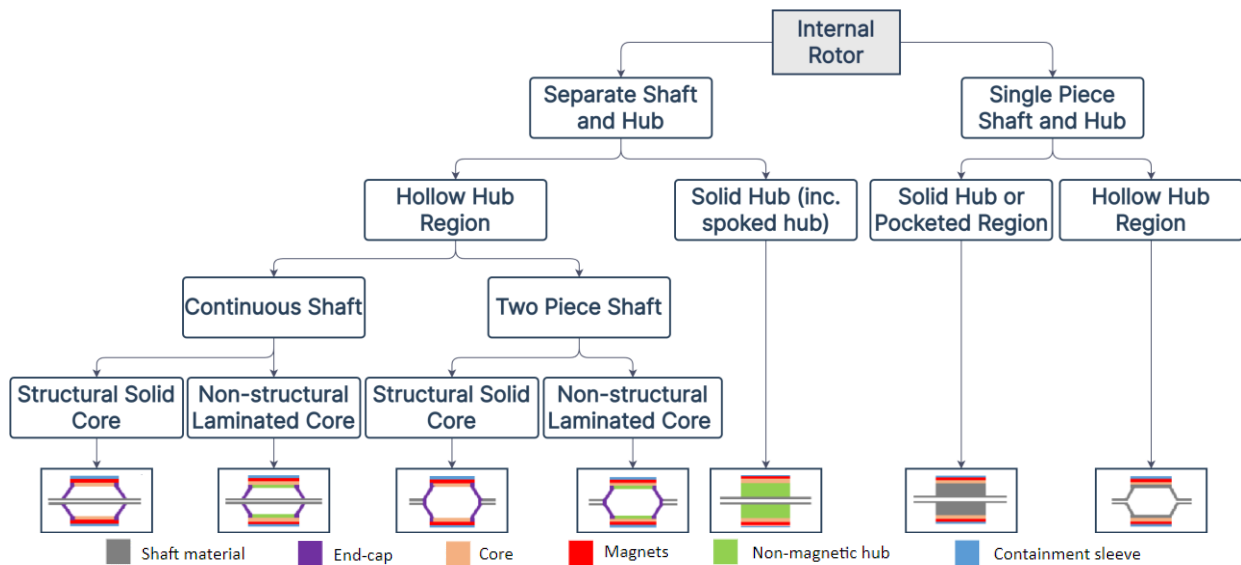
**FIGURE 3** Proposed taxonomy for internal permanent magnet rotors

[41], and this paper will build on a similar structure of using specific criterion to probe component details.

## III. Methodology development

The vast majority of electrical machines are manufactured as stand-alone machines with their own bearings and an all-encompassing casing. These stand-alone machines are then put to use by fixing the casing to some surrounding structure, typically through mechanical fasteners in combination with feet, flanges or lugs, and connecting the output shaft to the load via some form of coupling. In contrast, some machines are highly integrated with another mechanical system, such as internal combustion engines, and share many structural components including the shaft. Stand-alone machines tend to offer the most design freedom in terms of rotor design providing the drive-end of the rotor shaft is capable of being connected to the load with the preferred coupling type.

Traditionally, electrical machines have been designed focusing on the electrical, mechanical, and thermal performance. The design is then iterated to optimise for the performance criteria, with this finalised design then passed onto a manufacturer to fabricate. Since the manufacturing constraints have not been taken into consideration during the design, it often happens that changes are required to be made to the optimised design to make it manufacturable, leading to a non-optimal machine being manufactured.

Moreover, for several high-end applications, many future generation electrical machines are required to be lightweight, high power and operate reliably at relatively high rotational speeds. The likelihood of rotor dynamics problem occurring within the operating speed range of the machine is therefore increased. In contrast with other applications, an electrical machine shaft is subjected to a combination of mechanical and thermal loading, which can originate from manufacturing, assembly processes and during operation. This includes interference fits and compression from

containment sleeves, torque and thermal mismatch of materials in the assembly, as well as vibration [42].

If manufacturing is considered as an input variable to the design process, not only can these post-production changes be eliminated, but advantages of the manufacturing process can also be taken to produce a superior product. As an example, traditional methods of shaft design do not allow this iterative approach.

This paper will aim to develop a methodology for a fully integrated design and manufacturing process route.

The point of departure for the methodology is the identification of the possible design options. These design options can be identified systematically using a categorisation such as that shown in, FIGURE 3, which range from the standard through-shaft design, to a novel, one-piece hollow hub geometry. In order to differentiate between design choices, a first pass selection criteria was developed which conducts a trade-off between key aspects of potential manufacturing routes, including material properties associated to specific manufacturing methods. The inclusion of material data specific to manufacturing routes is a key element to this methodology as it will allow for the lightweighting of components when material strength can be increased during the manufacturing process. The final step before the modelling work is undertaken is to specify key properties of the design process in relation to the chosen methods of manufacture. All these points will be discussed in further detail below.

There have been several proposed taxonomies for classifying permanent magnet machine rotors such as [43]. However, these have been largely based on electromagnetic classification, in particular the arrangement of the rotor magnets. The taxonomy shown in FIGURE 3 is focussed on the mechanical configuration of the shaft/hub and rotor core for internal rotor machines. The myriad variation in the specific arrangement of magnets, i.e. whether they are

surface mounted, inset or interior magnets are not considered in this classification and indeed all three of these magnets configurations could be applied to all the rotor geometries of FIGURE 3. The schematic geometries shown in FIGURE 3 are highly simplified and in practice, many geometric features such as steps in shaft diameter to provide axial location, additional thin-walled endcaps to provide some axial retention of components. All the examples shown are based on hollow shafts but could in all cases be designed around solid shafts. Of the materials shown in the schematic representations of FIGURE 3, only the magnets and the core have important functional properties and the remaining materials can be selected entirely with regard to physical properties and thermal considerations. A summary of the candidate methods of manufacture and materials for each of the elements are shown in Table I and Table II, respectively.

From the taxonomy diagram, a list of potential manufacturing routes is generated and marked against each machine structure. In FIGURE 3, the structure types are numbered 1-7 from left to right, and comments are given in Table I on the feasibility of manufacturing the main structure (i.e. the rotor shaft, end caps, or combined hub region) with the specified method of manufacture. Comments are also made on the applicability of the individual manufacturing methods with respect to selected material types, shown in Table II.

The manufacturing routes and their applicability, shown in Table II, are limited in some cases to particular components within the rotor hub/shaft assembly. For example, radial forging is shown as applicable to all rotor designs, but the associated note is "for options 1, 2, 5, 6, radial forging is a feasible manufacturing method for the through shaft only. Alternative manufacturing options would need to be considered for the end caps and hub section (plus a joining method)". Every effort has been made to clearly state any restrictions on the applicability of the manufacturing methods in this paper.

The novelty of this methodology is the inclusion of manufacturing route-specific material data. A vast literature search was conducted to obtain public domain data on yield strength of the five materials considered in this paper, for the seven manufacturing routes, plus 'nominal' text book values. The inclusion of specific yield strength data in the design process allows for the component to be designed optimally based on the chosen method of manufacture. This will ensure that components are not over-specified which could lead to a detriment in cost or weight of the component, and will also

TABLE I
MANUFACTURING ROUTES VERSUS TAXONOMY OPTIONS

| | Forged solid bar + machining | Radial forging | Metal spinning | Extrusion + machining | Additive manufacture | Casting + machining | Centrifugal casting |
|---|---|---|---|---|---|---|---|
| 1. Structural solid core | ✓✓ | ✓ (1) | ✓ (3) | ✓ | ✓ (6) | ✓ (7) | ✗ (8) |
| 2. Non-structural laminated core | ✓✓ | ✓ (1) | ✓ (3) | ✓ | ✓ (6) | ✓ (7) | ✗ |
| 3. Structural solid core | ✓✓ | ✓ (2) | ✓ (3) | ✗ | ✓✓ | ✓✓ | ✗ |
| 4. Non-structural laminated core | ✓✓ | ✓ (2) | ✓ (3) | ✗ | ✓✓ | ✓✓ | ✗ |
| 5. Solid hub (inc. spoked hub) | ✓ | ✓ (1) | ✗ | ✗ | ✓ (6) | ✓ | ✓ (9) |
| 6. Solid hub or solid pocketed hub | ✓ | ✓ (1) | ✗ | ✓ (4) | ✓✓ | ✓ | ✓ (9) |
| 7. Hollow hub region | ✗ | ✓ | ✗ | O (5) | ✓ | O | O |
| Notes | ✓✓- Currently done in practice, O - Requires more information, | | | ✓- Not currently done in practice, but achievable ✗ - Not technically feasible | | | |

*(1) For options 1, 2, 5, 6, radial forging is a feasible manufacturing method for the through shaft only. Alternative manufacturing options would need to be considered for the end caps (plus a joining method)*
*(2) Radial forging would be feasible for the end shaft sections of this design, but would not be economically viable if the shaft is not long in length*
*(3) Metal spinning could be considered in this design for the end caps, but a joining technique would need to be considered the join the spun end caps to the through shaft*
*(4) It could be possible to extrude a single-piece tube but with different outer diameters, but this would require further development*
*(5) Extrusion of the hollow pocketed region could be feasible depending on the shape and thickness of the material*
*(6) Extrusion could potentially be used for the solid hub and/or the spoked hub but availability of tooling/press would be dependent of outer diameter of the hub*
*(7) Additive manufacturing would unlikely to be a cost effective method of manufacture for the shaft, but could be used for the end caps in conjunction with another manufacturing method of the shaft (depending on size and complexity)*
*(8) Casting could be considered in this design for the end caps, but a joining technique would need to be considered the join the cast end caps to the through shaft*
*(9) Centrifugal casting is not viable as the dimensions of the shaft are too small*
*(10) Centrifugal casting could be considered for this design but there would be a limit on the size of the hub inner diameter*

**IEEE** *Access*
Multidisciplinary : Rapid Review : Open Access Journal

TABLE II
MANUFACTURING ROUTES VERSUS MATERIAL SELECTION

| | Forged solid bar + machining | Radial forging | Metal spinning | Extrusion + machining | Additive manufacture | Casting + machining | Centrifugal casting |
|---|---|---|---|---|---|---|---|
| Titanium | ✔✔ | ✔✔ | ✔ (11) | ✘ | ✔✔ | ✔ (12) | ✘ |
| Steel | ✔✔ | ✔✔ | ✔ | ✔✔ | ✔✔ | ✔✔ | ✔✔ |
| Aluminium | ✔✔ | O | ✔ | ✔✔ | ✔✔ | ✔✔ | ✘ |
| Inconel | ✔✔ | ✔✔ | ✔ | ✔ (13) | ✔✔ | ✔ (12) | ✔ (12) |
| Magnesium | ✔ (14) | ✔ (14) | O | ✔ | ✔✔ | ✔ | ✔ |
| Notes | ✔✔- Currently done in practice, O - Requires more information, | | | ✔- Not currently done in practice, but achievable ✘ - Not technically feasible | | | |

(11) Due to the microstructure of Titanium, spinning needs to be performed hot (approx. 800-1000 °C)
(12) Casting on Inconel and Titanium is possible, but is often done in vacuum which increases cost and reduces possible geometries and sizes
(13) Extrusion of Inconel- this is feasible but readily available product sizes are limited
(14) Magnesium forging is more difficult than other metals, especially because the die set needs to be maintained at a specific temperature range

lead to optimal decision-making on choice of manufacturing route, ensuring that the full benefits of a particular method can be utilised. Table III summarises the yield strength for specific alloys and manufacturing routes.

The inclusion of material data specific to manufacturing routes is a key element to this methodology as it will allow for the lightweighting of components when material strength can be increased during the manufacturing process, e.g. through the use of cold forming processes. The final step before the modelling work is undertaken is to specify key properties of the design process in relation to the chosen methods of manufacture. For example, the minimum wall thickness achievable, the tolerances and component runout values, and any design criteria that need to be considered, i.e. min forming radii, minimum length of component. It is important to understand these constraints prior to the design stage as it allows for the engineer to optimally design the component for a specific method of manufacture.

Once the general methodology described above has been used to down-select potential options, the following staged process will be used to determine the information which will inform the modelling section of the methodology.

- *Stage 1*: Option selection; choice of options to take forward, with design profile and manufacturing route identified.
- *Stage 2*: Sketch of component; high level of detail, generalised geometry determined.
- *Stage 3*: Key design constraints determined; each design individually may require constraints on one or more of the features.
- *Stage 4*: Key manufacturing constraints determined; each design will have at least one manufacturing method with appropriate constraints.
- *Stage 5*: Combination of design and manufacturing constraints; combination of the output of steps 3 and 4, presented as a combined set of criteria to input into the modelling work.

It is important that each stage includes a detailed assessment to ensure that potential solutions are not overlooked,

TABLE III
MANUFACTURING ROUTES VERSUS MATERIAL PROPERTIES (YIELD STRESS)

| Method of manufacture | Titanium | Steel | Aluminum | Inconel | Magnesium |
|---|---|---|---|---|---|
| 'Nominal' text book values | 828 MPa [44] (Ti-64) | 1400 MPa [45] (Maraging Steel) | 260 MPa[46] (AL6082) | 1100 MPa [47] (IN718) | 165 MPa [48] (AZ31B) |
| Forged Solid Bar + Machining | 940 MPa [49] (Ti-64) | 1420 MPa [27] (Maraging Steel) | 170 MPa [50] (AL6082) | 1192 MPa [24] (IN718) | 169.9 MPa [51] (AZ31) |
| Radial Forging | 1380 MPa [24] (Transage 129) | 1007 MPa [52] (High strength alloy steel) | 330 MPa [53] (AL6082) | 1180 MPa [54] (IN718) | 163 MPa [55] (ZK60) |
| Metal Spinning | 925 MPa [26] (Ti-64) | 372 MPa [56] (SS 304) | 230 MPa [57] (AL7050) | 594 MPa [58] (IN625) | 310 MPa [59] (AZ31) |
| Extrusion + Machining | 275 MPa [60] (Ti grade 2) | 210 MPa [28] (SANMAC 304) | 295 MPa [61] (AL6082) | 276 MPa [62] (IN718) | 256 MPa [63] (AZ31) |
| Additive Manufacturing | 736 MPa [64] (Ti-64) | 590 MPa [65] (Austenite) | 260 MPa [65] (AlSi12) | 600 MPa [66] (IN718) | 95 MPa [67] (AZ31B) |
| Casting + Machining | 883 MPa [25] (Ti-64) | 619 MPa [68] (SS 316L) | 60 MPa [50] (AL6082) | 940 MPa [24] (IN718) | 92.9 MPa [69] (AZ91) |
| Centrifugal Casting | 950 MPa [70] (Ti-64) | 205 MPa [71] (MTEK304/L) | 150MPa [72] (AL356-SiC FGMMC) | 760 MPa [71] (MTEK718) | 150 MPa [73] (AZ31) |

however, the critical stage of the methodology is the combination of requirements in stage 5. For example, let the wall thickness of the component be considered. For the design stage, this requirement would likely take the form of the minimum wall thickness necessary for the component to withstand the forces exerted during operation, and for the chosen manufacturing route there will also be a minimum achievable thickness. When combining these two requirements, the larger of the two would be taken as the final component thickness. The combination of information from the design and manufacture of the component is the critical step, as this ensures the component is not using a manufacturing route or material type where the full benefits cannot be realised. This will be discussed in further detail with an example in the next section.

When compiling the list of manufacturing constraints, it is also important to be aware of the type of machine that could be used for the size of component being considered. For example, Table IV provides a summary of the design and manufacturing constraints that should be considered when a single-piece rotor with a hollow hub region is manufactured using radial forging. In this table, limits have been placed on geometrical features such as wall thickness and achievable diameters of both the hub and shaft. These limits have been imposed due to physical constraints of a particular radial forge- the GFM SKK10R- which was chosen as an appropriate machine for this size of component. This type of machine is used extensively in the automotive industry to forge drive shafts and rotor shafts, especially those with varied inner out outer diameter profiles [74]. Larger radial forges are available from various suppliers, but the larger machines are typically used to forge large diameter bar to smaller diameter bar which is then used in subsequent processes.

One of the main difficulties in compiling information such as that in Table IV is having access to the information on specific manufacturing processes. Unlike developing the electromagnetic or mechanical constraints which have associated equations, − will be discussed in future sections − the manufacturing constraints rely on direct experience or company know-how. There are several ways that this gap in knowledge can be overcome. For larger companies, internal design guides are often produced to guide engineers on the limits of specific manufacturing routes when designing new components. These design guides will typically include many of the same considerations which have been captured in Table IV with additional worked examples for specific components within the company catalogue.

In a more general setting, there have been several networks of research centres set up across the world to assist with bridging the gap between component designers and potential manufacturers. In the UK, the Catapult network − and more specifically for this application, the High Value Manufacturing Catapult − were set up to "bridge the gap between research and industry" and "tackle the biggest challenges that society and industries face today" [75]. Germany has a similar network of applied research centres

through the Fraunhofer-Gesellschaft organization [76], which aims to prioritise "key future-relevant technologies and commercializing its findings in business and industry", while the United States of America fund the National Laboratories [77] that addresses "large scale, complex research and development challenges with a multidisciplinary approach". Each of these research networks have specific groups or centres which focus on transitioning manufacturing-based research from academia to industry, and developing links that allow the experience from manufacturing to feed back to product designers.

TABLE IV
SUMMARY OF DESIGN AND MANUFACTURING CONSIDERATIONS AND CONSTRAINTS FOR A SINGLE-PIECE ROTOR MANUFACTURED USING RADIAL FORGING

| Single-Piece Rotor, Radial Forging | Design Considerations | Manufacturing Constraints |
|---|---|---|
| **Constraint 1:** Wall Thickness | Initially based on analytical design (section mechanical modelling) and further optimised through numerical analysis | Min approx. 1.5 mm* Max approx. 12 mm* |
| **Constraint 2:** Transition Slope of End Cap | Determined by bearing position, light- weighting and sufficient axial stiffness of the end cap | Slope between 0 and 75 degrees |
| **Constraint 3:** Ratio of Diameters | Finalised during modelling | Outer diameter ratio 1:5 (min : max) |
| **Constraint 4:** Diameter of Hub | Determined by the electromagnetic requirement | Maximum 125 mm* |
| **Constraint 5:** Diameter of Shaft | Outer diameter based on the available size of bearing and the inner diameter initially through the analytical design | Minimum 20 mm* |
| **Constraint 6:** Transition radii (fillet) | Radius between two adjacent steps must be larger than 0.2d to avoid stress concentration | 5-10 mm (dependent on tooling design) |
| **Constraint 7:** Material Selection | Combination of manufacturing route and material selection (see Table II) | Titanium, Steel, Inconel, Magnesium |

* Values based on using a GFM SKK10R radial forge, an appropriate size of machine for the size of the component

For the manufacturing constraints stated in Table IV every effort has been made to include the key points of note, however, when defining the constraints, there will always be implicitly imposed constraints which are not stated outright. For example, explicit constraints have been placed on the wall thickness, ratio of diameters, and shaft diameter. However, all of these aspects will inevitably lead to implicit constraints on tolerances on individual components, material movements during forming operations, and tolerance stack up during assembly.

## IV. Mechanical modelling and design

FIGURE 3 gives an overview of the comparative modelling of different rotor concepts. There are often two initial starting points for the analysis: (a) a definition of the electromagnetically active design, including dimensions and material properties and (b) a definition of rotor concept(s) to be modelled. Many of the leading dimensions of the rotor are set by electromagnetic considerations, e.g. overall rotor diameter and axial length of the active region. However, there are some elements that are dictated purely by mechanical and structural considerations such as shaft diameter and wall thickness of tubular structures. In order to establish initial estimates of these structural elements it is commonplace to fall-back on well-established analytical design and sizing equations.

Once the rotor concepts have been defined, a smaller subset of those concepts can be chosen for further study. This process is often qualitative, based on experience or driven by initial small studies. Many of these rotor concepts have multiple different manufacturing routes (both in terms of forming and assembly). The choice of manufacturing routes can affect global and local material properties and dimensional tolerances as well as manufacturing cost and time. This can mean that the evaluation of rotor concepts can be a matrix with topology and manufacturing routes being the two axes. Therefore, the design space is expanded to the combination of method of manufacturing and metallic material with mechanical properties influenced by the particular Method of Manufacture (MoM).

In this contribution the high-level aspects of the developed methodology on manufacturing-oriented design of rotor assembly is discussed. To this end, the success criteria is considered as achieving the weight reduction with a qualitative cost assessment in relation to the required MoM and choice of material using Table II. As per FIGURE 2, in order to embed the manufacturing in the rotor design, a global design procedure is required, in which the mechanical modelling parameters associated with rotor assembly components are initially determined. This initial design procedure is called analytical design in this work. The analytical design derives the dimensions and wall thicknesses of rotor components based on the properties of the selected metallic material associated with the specific MoM. The analytical design should also take account of the manufacturing and assemblage constraints such as minimum/maximum viable wall thickness, shaft outer radius in relation to available bearings, imposed stresses due to assemblage interference fit, etc. This procedure will present a first-pass at establishing a comparison between the options of the rotor's design for manufacturing to achieve the success criteria at the initial design stages. To the best of knowledge of the authors such procedure does not exist, as such this work will also contribute to the state-of-the-art from this perspective too. The procedure to obtain the analytical design is presented in the following section.

### A. Procedure to obtain initial design of rotor components

Here the aim is to lay out a straightforward analytical procedure to establish the initial design of rotor various components, including (wall) thickness of shaft, end cap, rotor hub, rotor core and sleeve as well as selection of the bearing. With respect to the selected rotor topology from the proposed taxonomy diagram, different set of components under slightly different loading conditions are required to be analysed. However, the design procedure for various rotor components is similar. Since the rotor components undergo a combination of stress contributions, a failure criterion for design is adopted firstly. The widely used criteria such as Tresca and Von Mises can be adopted, depending on the used material whether brittle (e.g. for cast metals) or ductile respectively. Since most of the manufacturing processes within the previous sections are applicable to ductile metallic material, the Von Mises is chosen, without loss of generality though.

For a three dimensional element in a cylindrical coordinate system the following stress components will act on different surfaces of element volume, which are hoop, radial, axial and shear stresses. The scope of this paper is focused on the applications in electrical machines where the axial stress (normally due to thrust force) contribution is not a significant design issue. A simplifying assumption of a thin cylinder is made, which allows the radial stress to also be set-aside. This is due to the fact that for the large ratios of component's diameter to thickness, which holds for rotor hub, core and sleeve, the thin cylinder theory's error is negligible [78]. According to thin cylinder theory, the hoop stress of a rotor component is expressed as [78].

$$\sigma_h = P D_O / 2t, \tag{1}$$

where $P$ is the imposed pressure and $D_O$ and $t$ stand for the component's outer diameter and wall-thickness. The imposed pressure can be either from an applied interference fit and sleeve pretension pressure or self-loading imparted due to the component's angular speed.

The shear stress imposed by the torque $T$ at a cross section of a rotor component is calculated as,

$$\tau = K_T T \, r / J, \tag{2}$$

with the polar second moment of area $J = \pi(D_O^4 - D_I^4)/32$ at a given cross section and $r$ denoting the radial distance of a point on the cylindrical rotor component. An appropriate load partial safety factor for torque, $K_T$, is also considered. Note that the inner diameter can be related to the outer diameter through the wall thickness, i.e. $D_I = D_O - 2t$.

Therefore, ignoring the axial and radial stresses, the failure criterion based on component's Von Mises stress, $\sigma_{v_{comp}}$ can be obtained through the following relations, with the hoop and shear stresses being determined for any specific rotor component.

$$\sigma_{v\,comp} \leq \frac{\sigma_y}{SF} \qquad (3)$$

$$\sigma_{v\,comp}^2 = \sigma_h^2 + 3\tau^2, \qquad (4)$$

in which $\sigma_y$, $\sigma_h$ and $\tau$ refer to the components' yield stress, hoop and shear stresses, and $SF$ is the material's partial safety factor [79] ($SF = 1.5$ in this paper). Appropriate values for safety factors are available in different standards. The reader is referred to the standard relevant to the specific applications. From the second of the above equations the inner radii (diameters) of each component can be written in terms of the wall thickness. As such, the thickness can directly be found such that it satisfies the failure criterion (the first of above equations). The flowchart in FIGURE 4 summarises the initial design procedure. In the following, the

pressure, which alleviates the hoop stress, negligible though due to the sleeves light weight. The sleeve's thickness is then determined so that the hoop stress (equation (1)) due to the combination of the mentioned pressures fulfils the failure criteria, given the yield tensile stress of the sleeve's composite material.

### C.   Hollow shaft stress analysis and design

Rotor shaft should primarily transfers the machine's torque. Shaft will undergo centrifugal forces that cause negligible amount of hoop stress ($\sigma_{sw}$), as shaft's cross sectional radius is relatively small. Consequently, the shear stress ($\tau_s$) due to the applied torque is the design driver. It is important to note that increasing the outer diameter of the shaft is beneficial to reducing the shear stress as its polar moment of area will rapidly grow, however, the outer diameter has to be selected with respect to the availability of the proper bearing.

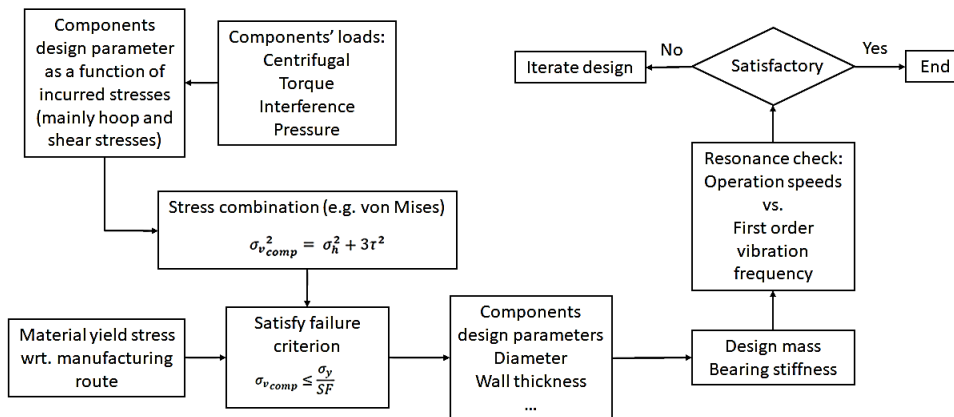Shaft's outer diameter should be determined such that the



**FIGURE 4  Flowchart of initial design procedure**

stress analysis for different rotor components is briefly described.

### B.   Sleeve design

Sleeve is required to hold the magnets in place at machine's extreme operational speed, $\omega_{max}$. Therefore, the sleeve's thickness is determined based the resulting hoop stress imposed due to an equivalent pressure, $P_{m_i}$, as a result of the magnet mass's centrifugal forces over the acting circumferential area:

$$P_{mi} = \frac{m_m R_m \omega_{max}^2}{S_m}, \qquad (5)$$

where $m_m$, $R_m$ and $S_m$ denoted the magnet's mass, radius and circumferential area. Similarly, radial pressures exist due to the dead weight of the inter-pole regions, $P_{ir}$ as well as the self-centrifugal loading of the sleeve [80].

The sleeve is pre-tensioned with an interference allowance that produces the mentioned required equivalent pressure. Note that the sleeve's self-loading acts in the opposite direction relative to the magnet and inter-pole

combined stresses fulfil the failure criteria, according to initial design flowchart and equation (4):

$$\sigma_{shaft} = \sqrt{\sigma_{sw}(d_{si})^2 + 3\tau_s(d_{si})^2} \leq \frac{\sigma_{ys}}{SF}. \qquad (6)$$

The above inequality is then solved to find the shaft inner diameter. In order to simplify the calculations, the shaft is conservatively assumed to be a thin cylinder which yields slightly higher wall thickness, therefore according to equation (1) and under the pressure caused by self-loading similar to equation (5) the shaft hoop stress becomes

$$\sigma_{sw} = \frac{\rho_s d_{so}^2 \omega^2}{4}. \qquad (7)$$

Using equation (2), the maximum shear stress to transmit the machine's torque is found as follows

$$\tau_s = \frac{16 K_{ol} T \, d_{so}}{\pi (d_{so}^4 - d_{si}^4)}, \qquad (8)$$

in which $K_{ol}$ and $T$ denote the overload factor and machine's mechanical torque, respectively. The flowchart in FIGURE 5 summarises the design procedure of the hollow shaft.
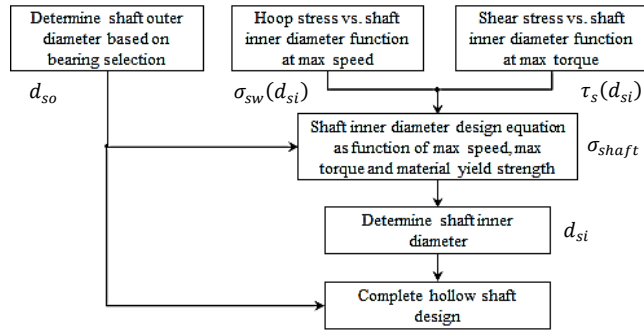


**FIGURE 5** Flowchart for hollow shaft design

### D.     Conical end cap design

The design principle of the end cap is considered similar to that of the shaft with the critical cross section at the connection point with the shaft. However, due to the variable cross section radii of the cone, its wall thickness can be further reduced from the shaft towards the hub connection point, leading to a tapered wall thickness. This will of course depend on the manufacturing machine's capability. Selection of the axial length of the conical ad cap and its impact on the design weight is further discussed in this section.

### E.     Rotor hub stress analysis and design

With reference to the proposed taxonomy diagram in FIGURE 3, the hoop stresses acting on the rotor hub depends on whether the hub consists of an outer electromagnetic core that sits on the internal hub or it is made up of a single rotor core (back-iron) as a structural element. In the former case that corresponds to the "single-piece shaft and hub/hollow hub region" (more briefly single-piece design), the electromagnetic core's thickness is determined to be the minimum thickness for avoiding the magnetic saturation. Then the inner hub is subject to two sets of compressive loads, causing a hoop stress, due to firstly the interference fit pressure (to attach the magnetic core onto the rotor hub) and secondly the sleeve's pre-tension pressure transmitted onto the hub through the rotor core. The interference fit pressure accounts for the surface normal force to provide the required friction between core and hub to transfer torque T:

$$P_{fr} = \frac{K_T T}{k_f R_{ho} S_{h_o}}, \tag{9}$$

where $K_T$, $k_f$ and $R_{ho}$ stand for torque partial safety factor, friction coefficient and the hub outer radius. The hub circumferential area is $S_{h_o} = 2\pi D_I L_a$, in which $L_a$ denotes the axial length of interference between hub and rotor core. To calculate the sleeve's transmitted pressure, a simplifying assumption is made, such that the pressure, $P_{h_m}$, is directly redistributed proportionate to the surface areas of the magnet

(magnet outer surface $S_m$) and hub outer surface $S_{h_o}$, namely $P_{h_m} = P_{m_i}(S_m/S_o)$, meaning that no pressure loss inside the magnets or the back-iron occurs. Note that $P_{m_i}$ is the required pre-tension in the sleeve to keep the magnets in place in the maximum operational speed of the machine according to equation (5).

The sleeve's transmitted pressure can be more accurately calculated through the application of thick cylinder theory to the compound cylinders. Nevertheless, the simplified redistributed pressure provides conservative design pressure that is of acceptable accuracy for this initial design phase. Finally, the resulting compressive hoop stress (equation (1)) from the total pressure exerted on the hub, that is $P_h = P_{fr} + P_{h_m}$, can be defined as a function of the hub thickness:

$$\sigma_{ht} = -P_h \frac{R_{ho}}{t_h}. \tag{10}$$

Furthermore, there is a shear stress acting on the hub due to the machine's torque (equation (2)), also defined as a function of hub thickness by:

$$\tau_s = \frac{K_{ol} T}{2\pi R_{ho}^2 t_h}. \tag{11}$$

An adequate hub thickness $t_h$ is determined to satisfy the following inequality (equation (4)) with respect to the combined hoop and shear stresses against the hub material's yield stress subject to the material safety factor:

$$\sigma_{hub} = \sqrt{\sigma_{ht}^2 + 3\tau_h^2} \leq \frac{\sigma_{yh}}{SF}. \tag{12}$$

In case corresponding to the "separate shaft and hub/structural solid core" of taxonomy diagram (or more briefly three-piece design) where the hub is made of the single structural core the interference for pressure does not exist, as such, just the sleeve's transmitted pressure is present (i.e., $P_h = P_{h_m}$) that causes the hoop stress. Note that the hub's determined thickness will be added to the required electromagnetic thickness, to guarantee low stress levels within the active part of rotor hub. The flowchart in FIGURE 6 summarises the design procedure of the single-piece hub design.

### F.     Spoked hub design

Spoked hub, as the reference design, is the first step in trying to remove the excessive mass from the shaft-rotor assembly through introducing the ribs (spokes). The transition of the machine's torque from a smaller diameter shaft to a larger diameter rotor hub has traditionally been made through a lump of mass (also known as step). Alternatively, the ribs in the spoked design take over the mentioned role, whereas in a hollowed hub this transition piece is completely removed and replaced by the end caps.

The design procedure for the hub of this design is similar to that of the three-piece design variant. As such, the focus

here is drawn to the design procedure of the ribs. The main loads that a single rib has to transfer between the shaft and hub are the axial force $F_{rb_h}$ due to the pressure of the magnet sleeve acting on the rotor hub circumference and the shear force $F_{rb_T}$ under machine's torque transmitted to the central axis of the shaft by the ribs. These forces can also be considered per unit axial length of each rib, which makes no difference in the calculation of the rib thickness. FIGURE 7 illustrates a zoomed view of a single rib with its dimensions and acting loads corresponding to the spoked hub rotor assembly from FIGURE 1.
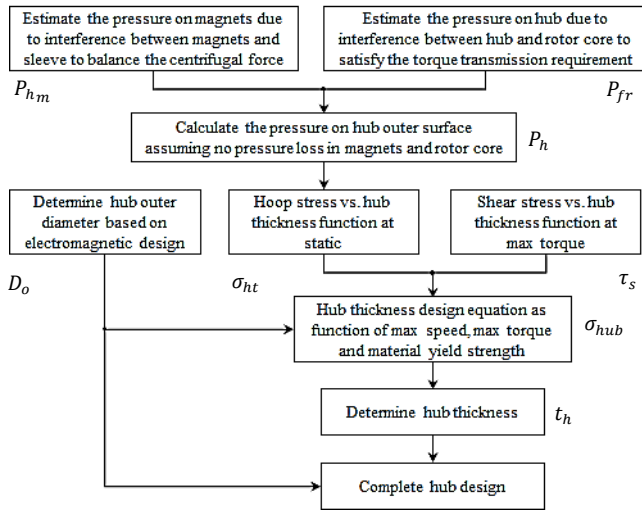


**FIGURE 6 Flowchart for single-piece hub design**

The above two forces are assumed to be equally distributed on all ribs and act on the tip of the ribs in a cantilever scenario, where the rib as a beam is clamped at the shaft connection. The axial force originates from the sleeve's pressure $(P_h)$ transmitted through the rotor hub and distributed onto the total number of ribs, $N_{rb}$. This force applies a normal stress, $\sigma_{rb}$, over the cross section of each rib:

$$\sigma_{rb} = \frac{F_{rbh}}{t_{rb}L_a} = \frac{2\pi R_{ho}P_h}{N_{rb}t_{rb}}, \tag{13}$$

in which $t_{rb}$ refers to the hub rib thickness. The shear force is resulting from the machine's torque with the torque arm towards the ribs root at shaft connection. This force applies a bending moment $M_{rb_T}$, maximum at the root of the cantilevered rib, namely at shaft connection point (see FIGURE 7). The cantilevered rib length, and the cross sectional height and width respectively equal to the moment arm $L_{rb}$, ribs' thickness $t_{rb}$ and hub's axial length $L_a$. Consequently, the maximum normal bending stress is determined as follows:

$$\sigma_{rbT} = \frac{F_{rbT}L_{rb}}{I_{rb}}(t_{rb}/2) = \frac{K_{ol}Tt_{rb}L_{rb}}{2N_{rb}(R_{ho}-t_h)I_{rb}}, \tag{14}$$

where the second moment of area of the hub rib is $I_{rb} = L_a t_{rb}^3/12$. Considering the hub thickness is small, the maximum imparted shear stress occurring at the neutral axis of rib cross section is one order of magnitude lower than the maximum normal bending stress. As such the shear stress is omitted in the stress combinations, so the rib thickness is determined so that the combined normal stresses fulfil the failure criteria (equation (3)). The number of ribs is a design parameter whose optimal choice requires an independent study that is outside the scope of this contribution. However, some high-level manufacturing considerations including the ease of machining/casting have been taken into account and as such there are eight ribs considered. For an increased design safety, it is assumed that no sleeve's pressure loss within the magnets occurs and the rotor hub doesn't compensate for any transmitted pressure either. Furthermore, an initial analysis showed that the shear stress contribution is negligible compared to normal stress in a cantilever scenario. In order to obtain the rib's thickness similar failure criterion is followed, in which the algebraic sum of normal stresses due to axial load and the bending stresses at rib's root is set to be less than yield strength, subject to safety factors.

$$\sigma_r = \sigma_{rb} + \sigma_{rbT} \leq \frac{\sigma_{yrb}}{SF}. \tag{15}$$

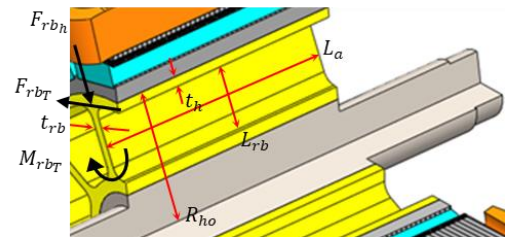The flowchart in FIGURE 8 summarises the design procedure of the spoked hub design.



**FIGURE 7 Dimensions and acting loads on a single rib in spoked hub design**

### G.    Selection of bearings and machine check from dynamics standpoint

The bearings are selected based on the shaft outer diameter. The bearing stiffness is then determined from the manufacturer's diagram with respect to the amount of imparted radial loads. The bearing radial loads comprises the rotor mass and the centrifugal force to the maximum allowable imbalance (As per ISO 21940-11:2016 [12], the permissible imbalance grade is G2.5) in relation to machine's extreme operating speed.

With the achieved mass of the rotor-shaft assembly (including the magnets) from the initial design procedure and the obtained bearing stiffness the low order vibration frequency is estimated, which is associated with the mass of the rotor assembly sitting on the flexible supports provided by the bearings [81]. This low order vibration frequency usually dominates the dynamic aspects of the design. Therefore, in conjunction with machines' operational speed

range, this vibration frequency is critical to be taken into account to avoid any resonance at the initial design phase. Accordingly, the required bearing stiffness, also with regard to the availability of desired diameter, will lead to the selection of the appropriate bearing. A good approximation of the first order bearing lateral mode of the rotor can be achieved using the fundamental definition of the natural vibration frequency of a simplified model. This model consists of the rotor as a lumped mass ($m_{tot_{rot}}$) supported by two bearings (each with stiffness $k_b$) that are considered as two springs in parallel with equivalent stiffness of $2k_b$:
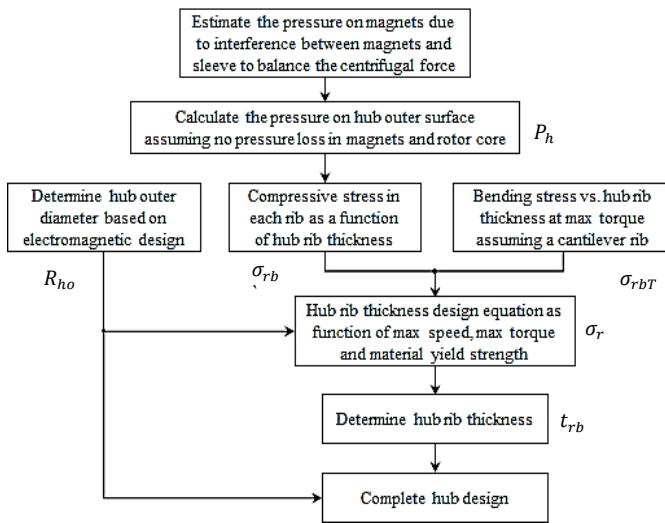


**FIGURE 8** Flowchart for spoked hub design

$$\omega = \sqrt{2k_b/m_{tot_{rot}}}. \qquad (16)$$

It is noted that the vibration modes of the rotor with deformable components and bearing are variable with respect to the machine's speed in the presence of the gyroscopic effects. As such, for a more detailed control of the machine's dynamics and stability associated with more complex higher modes a rotor dynamic analysis is usually carried out. This will need to be later computed numerically e.g., via finite element analysis to obtain the Campbell diagram of the machine. FIGURE *9* illustrates the complete procedure of rotor dynamics control.

### H. Lightweight design of Conical end caps and impact on rotor dynamics

The principal shaft and larger diameter hub, which supports the active rotor components, are coupled by conical sections, as seen in FIGURE 3, options 1-4 and 7. Designing these conical sections with discrete incrementally decreasing wall thickness, offers little in the way of mass saving, given the additional complexity in the manufacturing process. Therefore, the wall thickness of the conical sections, will inherit the designed thickness of the hub and principal shaft respectively, which results in a natural taper from the shaft

towards the larger diameter hub. Since the Polar Moment of Inertia of a cylindrical element is proportional to $diameter^4$, yet volume is only proportional $diameter^2$, the shear strength of the element increases at a greater rate than the mass (the superscripts designate the exponents). From simple geometrical considerations, decreasing the cone angle, and projecting the bearing supports further from rotor mass, results in a reduction in mass of the shaft / conical section combination. Projecting the bearings beyond the end windings of the machine will result in an increase in casing mass due to the extension of the casing to accommodate the bearing position. As a compromise between additional shaft and casing mass the axial position of the bearings will remain within the envelope of the end windings, for the purposes of this analysis. An analytical estimate of the critical frequency due to lateral deflection of the shaft assembly, using the Rayleigh method, is given by equation (17), where the static deflection, $y_i$, is calculated for every change of cross-section along the supported length. The maximum static deflection for a particular section of shaft is given by equation (18), where $a$ is the distance from the a bearing support to the applied transverse force, $l$ is the total distance between bearing supports, $I_a$ is the second moment of area and $E$ is the elastic modulus of the shaft material. In this case the transverse force could arise from a combination of mass and electromagnetic forces. If this calculated value of critical frequency exists within 120%  [19] of the maximum operating speed of the machine, adjustments in bearing position will be made to reduce the span of the bearing supports and reduce the critical frequency (or vice versa), albeit at the expense of additional shaft mass (in the conical sections).

$$N_c = \frac{30}{\pi} \sqrt{\frac{g \sum_i^m F_i y_i}{\sum_i^m F_i y_i^2}} \qquad (17)$$

$$y_{i,max} = \frac{F_i a^2 (l-a)^2}{3 E I_a l} \qquad (18)$$

These two equations are more applicable for the design options where there is a through shaft. Where no through shaft exists, equation (16) is an easier way to estimate the first critical vibration mode which, in most cases, is often dominated by bearing stiffness.

### V. Case study

This section demonstrates the implementation of the proposed methodology. At this stage, three different design options from the design taxonomy diagram are selected. Then the application of the developed procedure (FIGURE 2), in conjunction with Table I to Table III are demonstrated with the design and manufacturing consideration and constraints applied to integrate manufacturing from the initial stage of design. The design options include the rotor with spoked hub as design reference in comparison with
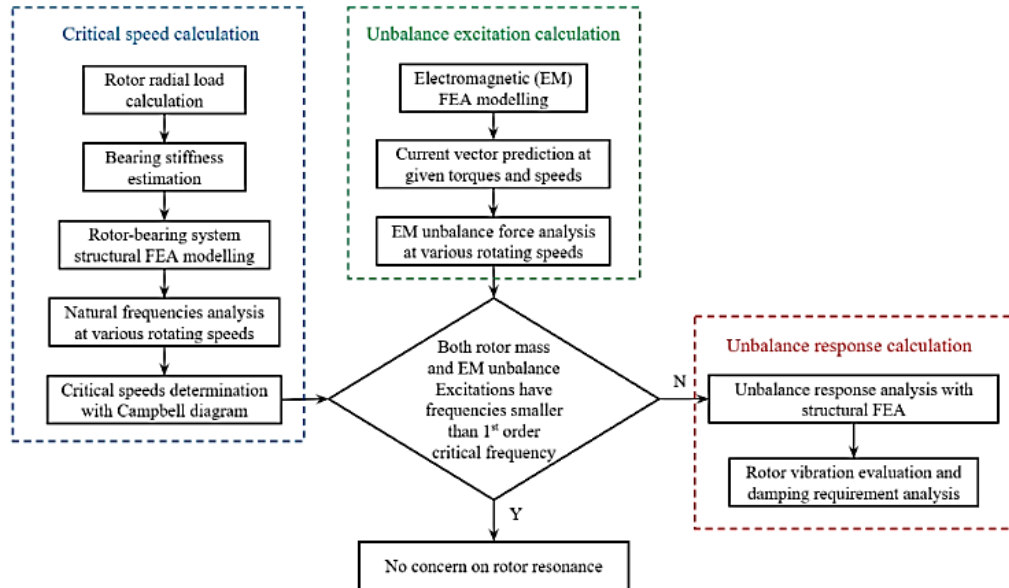
**FIGURE 9  Complete procedure of rotor dynamics control**

more modern choices of three-piece separate hub and shafts, and single-piece as respectively shown in FIGURE 10. For the sake of comparison, those manufacturing processes are adopted which are applicable to all design options, which are as follows: radial forging, casting & machining versus an undefined manufacturing procedure, utilising the nominal material properties. The manufacturing materials are titanium, aluminium, inconel and steel. Values from Table III are used for the initial design of rotor-shaft assembly in this paper, which provides the yield strength and density of the selected materials with the nominal values and those once they undergo the manufacturing process. It is presumed that the material's density will not considerably change as a consequence of the manufacturing method, and therefore the nominal density values are used everywhere.

The spoked hub and single-piece designs are considered to have rotor yoke lamination for the magnetic flux requirement, whereas the three-piece design with separate hub and shafts is assumed to have a solid rotor core with dual mechanical and magnetic performance. However, in order for an impartial comparison just the mass of the mechanical portion of the rotor hub is taken into account later for the analysis of the results. Due to the magnetic flux requirement, the rotor hub of the separate hub and shafts design has to only be made of steel, whereas the other designs do not need to bear this constraint. The machine's maximum speed and maximum torque are 12000 RPM and 380 Nm with a material's safety factor, SF and torque transmission safety factor $K_{ol}$ of both equal to 1.5. The friction coefficient for calculation of the interference in laminated rotor yoke is taken to be 0.2. The rotor yoke's inner diameter and axial length are taken to be 0.1103 and 0.092 m. The axial distance between shaft bearings is 0.160 m and is common for all three topologies in the case

study. The shaft projection beyond each bearing is 0.070 m and 0.017 m for the drive and non-drive ends of the machine respectively. This applies to the conventional through shaft with spoked hub, single-piece and three-piece design options. Table V,

Table VI, and Table VII below present the breakdown of component masses, as well as the total mass values, for all three design options. All shafts are considered to have a hollow profile after manufacturing.
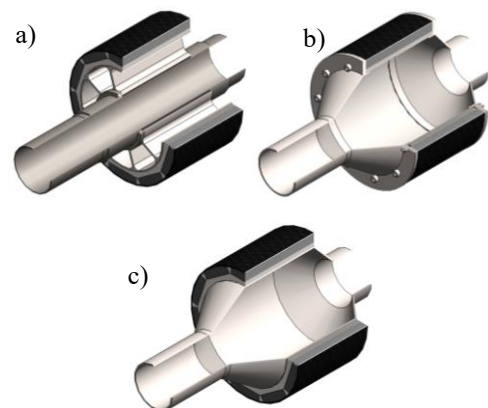


**FIGURE 10 Schematics for the three different design options considered in this case study: a) spoked hub, b) three-piece, and c) single-piece designs (Note: end caps are not shown on designs a) and c))**

The results using cast aluminium indicate that its properties are significantly degraded. The outer diameter of the shaft (0.05 m) is dominated by selection of the appropriate bearing, given the machine's speed and the imposed bearing radial force. Since the yield strength of cast aluminium

significantly degrades, this material is not suitable for the manufacturing of the shaft.

**TABLE V**
**SPOKED HUB MASS (KG)**

| Material Properties | Shaft | Hub | End cap | Total |
|---|---|---|---|---|
| *Nominal Material* | | | | |
| *Ti-64* | *0.085* | *0.296* | *0.124* | *0.504* |
| *Al-6082* | *0.170* | *0.463* | *0.074* | *0.707* |
| *Inconel-718* | *0.117* | *0.438* | *0.228* | *0.783* |
| *Steel-1045* | *0.411* | *1.161* | *0.217* | *1.788* |
| | | | | |
| *Radial Forging* | | | | |
| *Ti-64* | *0.050* | *0.200* | *0.124* | *0.374* |
| *Al-6082* | *0.132* | *0.378* | *0.074* | *0.584* |
| *Inconel-718* | *0.109* | *0.415* | *0.228* | *0.752* |
| *Steel-High Strength* | *0.122* | *0.446* | *0.217* | *0.785* |
| | | | | |
| *Cast and machining* | | | | |
| *Ti-64* | *0.079* | *0.281* | *0.124* | *0.484* |
| *Al-6082* | *-* | *1.692* | *0.074* | *-* |
| *Inconel-718* | *0.137* | *0.495* | *0.228* | *0.86* |
| *Steel-1045* | *0.200* | *0.655* | *0.217\** | *1.072* |

\* ALL END CAPS FOR THIS DESIGN ARE SET TO BE THE SAME WEIGHT AS THEY ARE STANDARD DISCS AND THEIR DESIGN HAS NOT BEEN OPTIMISED

**TABLE VI**
**SINGLE-PIECE HUB MASS (KG)**

| Material Properties | Shaft | Hub | End cap | Total |
|---|---|---|---|---|
| *Nominal Material* | | | | |
| *Ti-64* | *0.026* | *0.143* | *0.087* | *0.255* |
| *Al-6082* | *0.052* | *0.268* | *0.151* | *0.472* |
| *Inconel-718* | *0.036* | *0.199* | *0.125* | *0.360* |
| *Steel-1045* | *0.125* | *0.659* | *0.373* | *1.158* |
| | | | | |
| *Radial Forging* | | | | |
| *Ti-64* | *0.015* | *0.086* | *0.056* | *0.158* |
| *Al-6082* | *0.040* | *0.213* | *0.121* | *0.374* |
| *Inconel-718* | *0.033* | *0.186* | *0.119* | *0.337* |
| *Steel-High Strength* | *0.037* | *0.207* | *0.129* | *0.372* |
| | | | | |
| *Cast and machining* | | | | |
| *Ti-64* | *0.024* | *0.134* | *0.082* | *0.240* |
| *Al-6082* | *-* | *1.047* | *-* | *-* |
| *Inconel-718* | *0.042* | *0.233* | *0.144* | *0.418* |
| *Steel-1045* | *0.061* | *0.334* | *0.197* | *0.592* |

**TABLE VII**
**THREE-PIECE SOLID HUB MASS (KG)**

| Material Properties | Shaft | Hub | End cap | Total |
|---|---|---|---|---|
| *Nominal Material* | | | | |
| *Ti-64* | *0.026* | *-* | *0.087* | *0.634* |
| *Al-6082* | *0.052* | *-* | *0.151* | *0.725* |
| *Inconel-718* | *0.036* | *-* | *0.125* | *0.683* |
| *Steel-1045* | *0.125* | *0.522* | *0.373* | *1.020* |
| | | | | |
| *Radial Forging* | | | | |
| *Ti-64* | *0.015* | *-* | *0.056* | *0.235* |
| *Al-6082* | *0.040* | *-* | *0.121* | *0.324* |
| *Inconel-718* | *0.033* | *-* | *0.119* | *0.315* |
| *Steel-High Strength* | *0.037* | *0.163* | *0.129* | *0.329* |
| | | | | |
| *Cast and machining* | | | | |
| *Ti-64* | *0.024* | *-* | *0.082* | *0.370* |
| *Al-6082* | *-* | *-* | *-* | *-* |
| *Inconel-718* | *0.042* | *-* | *0.144* | *0.449* |
| *Steel-1045* | *0.061* | *0.264* | *0.197* | *0.522* |

FIGURE 11 provides the comparison of resulting components' mass for the rotor of spoked hub design, undergoing specific manufacturing routes. The total mass of varied rotor designs as a result of radial forging route is presented in FIGURE 12. As can be viewed, both design options and the manufacturing routes will impact on the components' achieved mass. It is worth noting that integration of manufacturing in the modelling in terms of design and material property variation can significantly alter the total mass, which demonstrates the application of the developed methodology being effective. Moreover, lighter weight design options can be obtained once the manufacturing route is considered. Some more specific results are also notable such as use of cast aluminium which doesn't seem to be an appropriate choice due to degradation of mechanical properties.
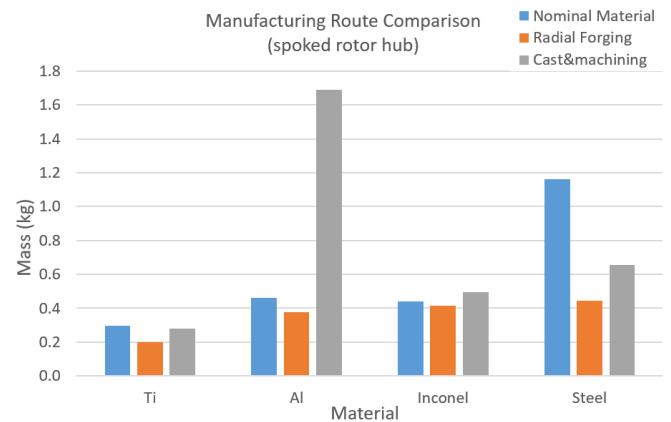
**FIGURE 11 Comparison of mass of the spoked rotor hub design when manufacturing specific material data is used**
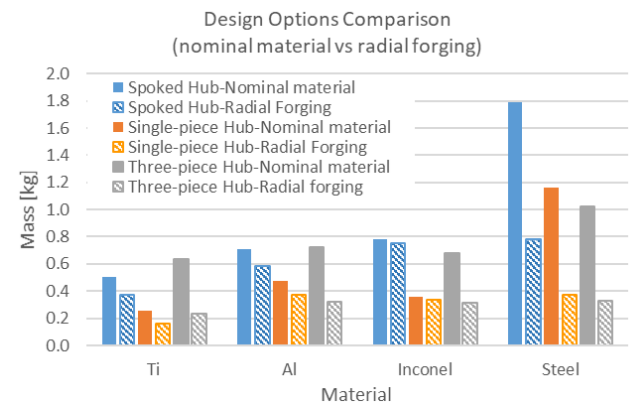
**FIGURE 12 Comparison of the total mass of various rotor designs for nominal material data and that specific to radial forging**

Associated with the results given in Table V,

TABLE VIII
FIRST ORDER VIBRATION FREQUENCY

| Material | Spoked hub | | Single piece hub | | Three-piece solid hub | |
|---|---|---|---|---|---|---|
| Properties | Hz | RPM | Hz | RPM | Hz | RPM |
| *Nominal Material* | | | | | | |
| *Ti-64* | *784* | *4.7E+04* | *819* | *4.9E+04* | *768* | *4.6E+04* |
| *Al-6082* | *759* | *4.6E+04* | *789* | *4.7E+04* | *757* | *4.5E+04* |
| *Inconel-718* | *750* | *4.5E+04* | *804* | *4.8E+04* | *762* | *4.6E+04* |
| *Steel-1045* | *655* | *3.9E+04* | *710* | *4.3E+04* | *724* | *4.3E+04* |
| | | | | | | |
| *Radial Forging* | | | | | | |
| *Ti-64* | *802* | *4.8E+04* | *834* | *5.0E+04* | *822* | *4.9E+04* |
| *Al-6082* | *774* | *4.6E+04* | *802* | *4.8E+04* | *809* | *4.9E+04* |
| *Inconel-718* | *753* | *4.5E+04* | *807* | *4.8E+04* | *810* | *4.9E+04* |
| *Steel-high strength* | *750* | *4.5E+04* | *802* | *4.8E+04* | *808* | *4.9E+04* |
| | | | | | | |
| *Cast and machining* | | | | | | |
| *Ti-64* | *787* | *4.7E+04* | *821* | *4.9E+04* | *802* | *4.8E+04* |
| *Al-6082\** | *-* | *-* | *-* | *-* | *-* | *-* |
| *Inconel-718* | *741* | *4.4E+04* | *796* | *4.8E+04* | *791* | *4.7E+04* |
| *Steel-1045* | *719* | *4.3E+04* | *773* | *4.6E+04* | *782* | *4.7E+04* |

\* CAST ALUMINIUM IS NOT SUITABLE TO MAKE SHAFT DUE TO ITS LOW STRENGTH

Table VI, and Table VII, the first order vibration frequency of different rotor options with a total mass contribution from active components of 2.47 kg are presented in Table VIII, according to equation (16). Note that the stiffness of 3.61e07 N/m is adopted for the three design options. Since the maximum operating speed of the case study machine is 10e3 RPM, there is no risk of resonance within the operating speed range of these design options, based on the results in Table VIII.

Once the initial design wall-thicknesses are derived, at this stage the manufacturing constraints with reference to Table IV need to be imposed. To demonstrate this step, the wall thickness is set to the minimum achievable one via using specific radial forging machines. Through a closer look into the obtained results any wall thickness value below the machine's capability of 1.5 mm is increased to this thickness threshold. Comparison of components' initial mass (initial) and once the constraint imposed (adjusted) reveals an interesting point in choosing more/less expensive material.

Table IX presents the detailed comparison for the obtained mass of shaft and hub in the spoked hub and single-piece design. Comparison between titanium and aluminium for the shaft's manufacturing in Table IX shows that after imposing this manufacturing constraint the choice of more expensive material (titanium) is not only providing no benefit in terms of weight reduction but is actually resulting in a heavier design. In this case, the benefits of the radial forging process, as well as the material benefits of choosing titanium, are not being fully optimised and are therefore not a suitable choice in this instance. Similar situations hold for the shaft being manufactured from inconel and steel. The same comparison demonstrates that either marginal weight reduction or heavier design is achieved when this constraint is applied for hub thickness. Nevertheless, it is noted that applying the manufacturing constraints highly depends on the specific case study – for example, the wall thickness directly depend the loads of a specific machine. Therefore, for each specific design, these constraints should be laid out

at the initial stages properly. Individual manufacturing processes can provide advantages to the design and performance of a final component, but it is important that they are applied appropriately. In this analysis, the aim is to demonstrate the impact of such constraints through this specific application to ensure that for a specific design the optimal solution is achieved in both design and manufacturing aspect.

TABLE IX
DESIGN MASS COMPARISON BETWEEN DIFFERENT MATERIALS AND MANUFACTURING CONSTRAINTS

| Radial | Shaft mass (kg) | | Hub mass (kg) | |
|---|---|---|---|---|
| Forging | Initial | Adjusted | Initial | Adjusted |
| *Spoked hub design* | | | | |
| *Ti-64* | *0.050* | *0.279* | *0.200* | *0.347* |
| *Al-6082* | *0.132* | *0.162* | *0.378* | *0.378* |
| *Inconel-718* | *0.109* | *0.514* | *0.415* | *0.666* |
| *Steel-1045* | *0.122* | *0.487* | *0.446* | *0.660* |
| | | | | |
| *Single-piece design* | | | | |
| *Ti-64* | *0.015* | *0.085* | *0.086* | *0.215* |
| *Al-6082* | *0.040* | *0.049* | *0.213* | *0.213* |
| *Inconel-718* | *0.033* | *0.157* | *0.186* | *0.396* |
| *Steel-1045* | *0.037* | *0.149* | *0.207* | *0.376* |

## VI. Conclusion

This paper presents the outcome of research work which has identified and addressed the gap in integration of the manufacturing methods with design of non-active (structural) components of electrical machines for their lightweighting with application to aerospace and automotive. In order to address this need, this paper took a novel approach to develop a methodology in which a wide range of design and manufacturing options as well as impact of manufacturing methods and choice of material on the mechanical design are all taken into account from the beginning up to the end of the design procedures. A detailed process is also provided to enable achieving an initial design of various components where the material properties and constraints specific to each method of manufacturing are

IEEE Access
Multidisciplinary : Rapid Review : Open Access Journal

embedded into the mechanical design. This is to prevent later modifications that are normally required to make the design compatible with the method of manufacturing. It should be noted that the design and manufacturing of electrical machines in some specific areas such as in aerospace is a delicate process, in which any unforeseen changes can spoil the main design purpose or the aimed benefits.

Furthermore, the implementation of the developed methodology for an aerospace electrical machine case study is demonstrated. As it is the aim of this work, the results indicate the promising potential of the integration of manufacturing and design, which can be unlocked by means of the proposed methodology. Within the case study, values were computed for the mass of the spoked rotor hub for various materials and manufacturing routes. It was shown that there is a clear potential for lightweighting if an appropriate method of manufacture is adopted, with respect to both material and component design. For example, if radial forging is selected for a steel spoked hub then its mass can be reduced to less than 40% of the mass using the nominal material properties. In contrast, if a standard casting route is taken for an aluminium spoked hub then the final mass is increased to almost four times the mass when using nominal aluminium properties, emphasising the importance of knowledge about manufacturing routes and their impact on the mass of the final product.

In addition, as the results indicate the manufacturing constraints also have to be taken into account to obtain a realistic potential for lightweighting. For example, a constraint on the minimum achievable wall thickness through radial forging limits the lightweighting gain once a more expensive material, such as inconel, is chosen. The mass of an aluminium spoked hub remains unchanged due to implementation of minimum wall thickness, but if inconel is chosen instead then the wall thickness constraint has to be applied, which yields an increase of almost 60% in the spoked hub mass. A similar quantitative analysis of the results can also be made for the single piece and three piece solid hub design options.

This paper is the way of opening a new door to a new area of research and the authors admit that there are significant amounts of research opportunities remaining in this area which need to be addressed. An immediate follow-up of this work will be an in-depth computational modelling and mechanical analysis through which optimal components' design for the sake of an accurate lightweighting assessment can be obtained. Further work will include the adaptation and enhancement of the developed methodology for other applications such as wind turbines with cost assessment integration to address cost-effectiveness in manufacturing of large generators such as those in directly driven generator systems.

## VII. Funding

## VIII. References

[1] Balachandran A, Boden M, Sun Z, Forrest SJ, Ede JD, Jewell GW. Design, construction, and testing of an aero-engine starter-generator for the more-electric aircraft. J Eng. 2019;2019(17):3474–8.

[2] Moghaddam RR. High speed operation of electrical machines, a review on technology, benefits and challenges. In: 2014 IEEE Energy Conversion Congress and Exposition (ECCE). IEEE; 2014. p. 5539–46.

[3] Armah SK. Preliminary design of a power transmission shaft under fatigue loading using ASME code. Am J Eng Appl Sci. 2018;11(1):227–44.

[4] Fang H, Qu R, Li J, Zheng P, Fan X. Rotor design for high-speed high-power permanent-magnet synchronous machines. IEEE Trans Ind Appl. 2017;53(4):3411–9.

[5] Zhang F, Du G, Wang T, Liu G, Cao W. Rotor retaining sleeve design for a 1.12-MW high-speed PM machine. IEEE Trans Ind Appl. 2015;51(5):3675–85.

[6] Boglietti A, Cossale M, Popescu M, Staton DA. Electrical machines thermal model: Advanced calibration techniques. IEEE Trans Ind Appl. 2019;55(3):2620–8.

[7] Nishanth F, Johnson M, Severson EL. A Review of Thermal Analysis and Management of Power Dense Electric Machines. In: 2021 IEEE International Electric Machines & Drives Conference (IEMDC). IEEE; 2021. p. 1–8.

[8] Shen J, Qin X, Wang Y. High-speed permanent magnet electrical machines—applications, key issues and challenges. CES Trans Electr Mach Syst. 2018;2(1):23–33.

[9] Zhao W, Wang X, Gerada C, Zhang H, Liu C, Wang Y. Multi-physics and multi-objective optimization of a high speed PMSM for high performance applications. IEEE Trans Magn. 2018;54(11):1–5.

[10] Jang S-M, Park H-I, Choi J-Y, Ko K-J, Lee S-H. Magnet pole shape design of permanent magnet machine for minimization of torque ripple based on electromagnetic field theory. IEEE Trans Magn. 2011;47(10):3586–9.

[11] Sergeant P, Van den Bossche A. Segmentation of magnets to reduce losses in permanent-magnet synchronous machines. IEEE Trans Magn. 2008;44(11):4409–12.

[12] 21940-11:2016 I. Mechanical vibration — Rotor

balancing — Part 11: Procedures and tolerances for rotors with rigid behaviour. 2016.

[13] GUO D, CHU F, Chen D. The unbalanced magnetic pull and its effects on vibration in a three-phase generator with eccentric rotor. J Sound Vib. 2002;254(2):297–312.

[14] Xu X, Han Q, Chu F. Review of electromagnetic vibration in electrical machines. Energies. 2018;11(7):1779.

[15] Zhuo M, Yang L, Yu L. The steady-state thermal effect on dynamic characteristics of gas turbine rotor considering contact effect. In: 2014 IEEE International Conference on Mechatronics and Automation. 2014. p. 981–6.

[16] Zheng M, Huang W, Gao C. Rotor stress and dynamics analysis of a high-speed permanent magnet machine for a micro gas turbine considering multiphysics factors. IEEE Access. 2020;8:152523–31.

[17] Tenconi A, Vaschetto S, Vigliani A. Electrical machines for high-speed applications: Design considerations and tradeoffs. IEEE Trans Ind Electron. 2013;61(6):3022–9.

[18] Sikanen E, Nerg J, Heikkinen JE, Tehrani MG, Sopanen J. Fatigue life calculation procedure for the rotor of an embedded magnet traction motor taking into account thermomechanical loads. Mech Syst Signal Process. 2018;111:36–46.

[19] Tong W. Mechanical design of electric motors. CRC press; 2014.

[20] Genta G. Dynamics of rotating systems. Springer Science & Business Media; 2007.

[21] Eastham JF, Profumo F, Tenconi A, Hill-Cottingham R, Coles P, Gianolio G. Novel axial flux machine for aircraft drive: design and modeling. IEEE Trans Magn. 2002;38(5):3003–5.

[22] Koch S-F, Peter M, Fleischer J. Lightweight design and manufacturing of composites for high-performance electric motors. Procedia CIRP. 2017;66:283–8.

[23] Jaen-Sola P, McDonald AS, Oterkus E. Lightweight design of direct-drive wind turbine electrical generators: A comparison between steel and composite material structures. Ocean Eng. 2019;181:330–41.

[24] Trosch T, Strößner J, Völkl R, Glatzel U. Microstructure and mechanical properties of selective laser melted Inconel 718 compared to forging and casting. Mater Lett. 2016;164:428–31.

[25] Saha RL, Jacob KT. Casting of Titanium and its Alloys. Def Sci J. 1986;36(2):121–41.

[26] Imamura Y, Ikawa K, Motoyama K, Iwasaki H, Hirakawa T, Utsunomiya H. An Experimental Study for the Development of Mandrel-Free Hot-Spinning for Large Size Titanium Alloy Plate Forming. J Eng Gas Turbines Power. 2019;141(3).

[27] ATi C-200TM/C-250TM/C-300TM/C-350TM Alloys [Internet]. ATI Metals; Available from: https://www.atimetals.com/Products/Documents/datasheets/stainless-specialty-steel/specialtysteel/ati_c-200-250-300-350_tds_en1_v1.pdf

[28] SANMAC 304/304L Hollow Bar Datasheet [Internet]. Sandvik; Available from: https://www.materials.sandvik/en/products/tube-pipe-fittings-and-flanges/tubular-products/hollow-bar/standard-sizes/

[29] Mei Z, He Y, Jing GUO, Wang X. Review on hot spinning for difficult-to-deform lightweight metals. Trans Nonferrous Met Soc China. 2015;25(6):1732–43.

[30] Brummer C, Eck S, Marsoner S, Arntz K, Klocke F. Laser-assisted metal spinning for an efficient and flexible processing of challenging materials. In: IOP Conference Series: Materials Science and Engineering. IOP Publishing; 2016. p. 12022.

[31] Li S, Li Y, Choi W, Sarlioglu B. High-speed electric machines: Challenges and design considerations. IEEE Trans Transp Electrif. 2016;2(1):2–13.

[32] Henke M, Narjes G, Hoffmann J, Wohlers C, Urbanek S, Heister C, et al. Challenges and opportunities of very light high-performance electric drives for aviation. Energies. 2018;11(2):344.

[33] Jaen Sola P, McDonald AS, Oterkus E. A lightweight approach for airborne wind turbine drivetrains. Eur Wind Energy Assoc EWEA 2015. 2015;1–9.

[34] Uddin MS, Morozov E V, Shankar K. The effect of filament winding mosaic pattern on the stress state of filament wound composite flywheel disk. Compos Struct. 2014;107:260–75.

[35] Daukaev K, Rassõlkin A, Kallaste A, Vaimann T, Belahcen A. A review of electrical machine design processes from the standpoint of software selection. In: 2017 IEEE 58th International Scientific Conference on Power and Electrical Engineering of Riga Technical University (RTUCON). IEEE; 2017. p. 1–6.

[36] Bramerdorfer G, Tapia JA, Pyrhönen JJ, Cavagnino A. Modern electrical machine design optimization: Techniques, trends, and best practices. IEEE Trans Ind Electron. 2018;65(10):7672–84.

[37] Lei G, Zhu J, Guo Y, Liu C, Ma B. A review of design optimization methods for electrical machines. Energies. 2017;10(12):1962.

[38] Domingues G, Márquez-Fernández FJ, Fyhr P, Reinap A, Andersson M, Alaküla M. Scalable performance, efficiency and thermal models for electric drive components used in powertrain simulation and optimization. In: 2017 IEEE Transportation Electrification Conference and Expo (ITEC). IEEE; 2017. p. 644–9.

[39] Domingues-Olavarria G, Marquez-Fernandez FJ, Fyhr P, Reinap A, Andersson M, Alaküla M. Optimization of electric powertrains based on scalable cost and performance models. IEEE Trans Ind Appl. 2018;55(1):751–64.

[40] Kuo T-C, Huang SH, Zhang H-C. Design for manufacture and design for 'X': concepts, applications, and perspectives. Comput Ind Eng. 2001;41(3):241–60.

[41] 8887-220:2010 B. Design for manufacture, assembly, disassembly and end-of-life processing (MADE) - The process of remanufacture. Specification. 2010.

[42] Ahmad HY, Bonnieman D. Fundamental Recommendations for the Design Configuration of Rotor Shafts for Use in Electric Motors and Generators. Procedia Eng [Internet]. 2016;160:37–44. Available from: https://www.sciencedirect.com/science/article/pii/S1877705816330958

[43] Liu X, Fu WN, Niu S. Optimal structure design of permanent magnet motors based on a general pattern of rotor topologies. IEEE Trans Magn. 2017;53(11):1–4.

[44] 6-4, 6-4 ELI & 6-4-.1Ru: Medium to high strength general-purpose alloys. Timet;

[45] Davis JR. ASM specialty handbook: tool materials. ASM international; 1995.

[46] Aluminum 6082-T6 [Internet]. MatWeb; Available from: http://www.matweb.com/search/datasheet_print.aspx?matguid=fad29be6e64d4e95a241690f1f6e1eb7

[47] Special Metals Inconel Alloy 718 [Internet]. MatWeb; Available from: http://www.matweb.com/search/DataSheet.aspx?MatGUID=94950a2d209040a09b89952d45086134&c

kck=1

[48] Magnesium AZ31B, Extruded Hollow Shapes [Internet]. MatWeb; Available from: Magnesium AZ31B, Extruded Hollow Shapes

[49] Sun Y, Zeng W, Han Y, Zhao Y, Wang G, Dargusch MS, et al. Modeling the correlation between microstructure and the properties of the Ti–6Al–4V alloy based on an artificial neural network. Mater Sci Eng A. 2011;528(29–30):8757–64.

[50] Mrówka-Nowotnik G, Sieniawski J. Influence of heat treatment on the microstructure and mechanical properties of 6005 and 6082 aluminium alloys. J Mater Process Technol. 2005;162:367–72.

[51] Stefanik A, Szota P, Mróz S, Bajor T DH. Properties of the AZ31 magnesium alloy round bars obtained in different rolling processes. Arch Metall Mater. 2015;60(4):3001–5.

[52] Yang Y, Fan L, Xu C. The microstructure, texture evolution and plasticity anisotropy of 30SiMn2MoVA high strength alloy steel tube processed by cold radial forging. Mater Charact. 2020;169:110641.

[53] Forcellese A, Gabrielli F. Warm forging of aluminium alloys: a new approach for time compression of the forging sequence. Int J Mach Tools Manuf. 2000;40(9):1285–97.

[54] Wang Z, Zhou D, Deng Q, Chen G, Xie W. The microstructure and mechanical properties of inconel 718 fine grain ring forging. In: 7th International Symposium on Superalloy. 2010.

[55] Zou J, Ma L, Jia W, Le Q, Qin G, Yuan Y. Microstructural and mechanical response of ZK60 magnesium alloy subjected to radial forging. J Mater Sci Technol. 2021;83:228–38.

[56] Ren CX, Wang Q, Zhang ZJ, Yang HJ, Zhang ZF. Enhanced tensile and bending yield strengths of 304 stainless steel and H62 brass by surface spinning strengthening. Mater Sci Eng A. 2019;754:593–601.

[57] Molladavoudi HR, Djavanroodi F. Experimental study of thickness reduction effects on mechanical properties and spinning accuracy of aluminum 7075-O, during flow forming. Int J Adv Manuf Technol. 2011;52(9):949–57.

[58] Maj P, Mizera J, Pieja T, Gancarczyk T, Dudek S, Sieniawski J. The development of metal spinning— new opportunities and possibilities. Inżynieria Mater. 2016;37(5):252–7.

[59]    Shirizly A, Felzenstein M. TUBE SPINNING OF MAGNESIUM ALLOYS.

[60]    Ti Grade 5 / Ti-6Al-4V / W-Nr.3.7164/65 [Internet]. Bibus Metals; 2021. Available from: https://www.bibusmetals.com/products/titanium-grade-5-6al-4v/

[61]    Extruded products [Internet]. The aluminium automotive manual; 2022. Available from: https://www.european-aluminium.eu/media/1539/aam-products-2-extruded-products.pdf

[62]    Nickel Alloys [Internet]. corrotherm; Available from: https://www.corrotherm.co.uk/grades

[63]    Chino Y, Hoshika T, Mabuchi M. Mechanical and corrosion properties of AZ31 magnesium alloy repeatedly recycled by hot extrusion. Mater Trans. 2006;47(4):1040–6.

[64]    Kasperovich G, Hausmann J. Improvement of fatigue resistance and ductility of TiAl6V4 processed by selective laser melting. J Mater Process Technol. 2015;220:202–14.

[65]    Herzog D, Seyda V, Wycisk E, Emmelmann C. Additive manufacturing of metals. Acta Mater. 2016;117:371–92.

[66]    Raghavan S, Zhang B, Wang P, Sun C-N, Nai MLS, Li T, et al. Effect of different heat treatments on the microstructure and mechanical properties in selective laser melted INCONEL 718 alloy. Mater Manuf Process. 2017;32(14):1588–95.

[67]    Takagi H, Sasahara H, Abe T, Sannomiya H, Nishiyama S, Ohta S, et al. Material-property evaluation of magnesium alloys fabricated using wire-and-arc-based additive manufacturing. Addit Manuf. 2018;24:498–507.

[68]    Şimşir M, Kumruoğlu LC, Özer A. An investigation into stainless-steel/structural-alloy-steel bimetal produced by shell mould casting. Mater Des. 2009;30(2):264–70.

[69]    Luo AA. Magnesium casting technology for structural applications. J Magnes Alloy [Internet]. 2013;1(1):2–22. Available from: https://www.sciencedirect.com/science/article/pii/S2213956713000030

[70]    Koeser O, Kalkunte B, Yang R, Hai N. Centrifugal casting of large ti-6al-4v structural components supported by process modelling. In: 71st Worl Foundry Congress. 2014.

[71]    Metaltek [Internet]. Available from: https://www.metaltek.com/alloys/

[72]    Rajan TPD, Pillai RM, Pai BC. Centrifugal casting of functionally graded aluminium matrix composite components. Int J Cast Met Res. 2008;21(1–4):214–8.

[73]    Liu JW, Peng XD, Chen DS, Yi HY, Yu YQ. Microstructure and mechanical properties of centrifugal casting of AZ31B magnesium alloy ring. Mater Res Innov. 2014;18(sup4):S4-169.

[74]    GFM [Internet]. Available from: https://www.gfm.at/radialschmiedemaschinen-automobilindustrie/?lang=en

[75]    Catapult, UK [Internet]. Available from: https://catapult.org.uk/about-us/why-the-catapult-network/

[76]    Fraunhofer, Germany [Internet]. Available from: https://www.fraunhofer.de/en.html

[77]    National Laboratories, USA [Internet]. Available from: https://www.energy.gov/national-laboratories

[78]    Hearn EJ. Mechanics of Materials 1: Introduction to the Mechanics of Elastic and Plastic Deformation of Solids and Structural Materials. 3rd ed. Butterworth-Heinemann; 1997.

[79]    Eckert C, Isaksson O. Safety margins and design margins: a differentiation between interconnected concepts. Procedia CIRP. 2017;60:267–72.

[80]    Kragh KA, Fleming PA, Scholbrock AK. Increased Power Capture by Rotor Speed–Dependent Yaw Control of Wind Turbines. J Sol Energy Eng [Internet]. 2013;135(3):31018. Available from: http://solarenergyengineering.asmedigitalcollection.asme.org/article.aspx?doi=10.1115/1.4023971

[81]    Friswell MI, Penny JET, Garvey SD, Lees AW. Dynamics of rotating machines. Cambridge university press; 2010.